P1.2 ISLAND-SCALE AIRFLOW AND THE MAUI VORTEX UNDER SUMMER TRADE-WIND CONDITIONS

DaNa L. Carlis*
Honolulu Weather Forecast Office, Honolulu, HI
and Howard University, Washington, DC

Yi-Leng Chen
University of Hawaii, Honolulu, HI

1. Introduction

Airflows over an isolated flow barrier in the subtropics are influenced by topography, the height of the trade-wind inversion (Leopold 1949), and upstream trade-wind conditions (Smolarkiewicz et al. 1988; Schar and Smith 1993; Chen and Feng 2001). For mountains with tops well above the trade-wind inversion, the inversion layer acts as a capping lid forcing the incoming air to divert around the mountains (Leopold 1949). In addition, the Froude number (Fr = U/Nh) is a useful parameter to characterize the behavior of the flow, where U is the flow speed, h is the height of the obstacle, and N (0.01 s^{-1}) the Brunt-Väisällä frequency. Smolarkiewicz and Rotunno (1989) showed that for Fr < 1, two counter-rotating vortices are generated baroclinically in the lee of the flow barrier in their model without considering the surface friction. Schar and Smith (1993) studied flow regimes based on Fr and the depth of the flow in comparison with the mountain height. The topography of Maui is dominated by two large mountains; Haleakala (height ~3,055 m) to the east and the West Maui Mountains (height ~1,764 m) (Fig. 1). The mountains are connected by a flat isthmus known as the Central Valley that is mostly sugar cane fields. Under normal (U ~ 7 m s^{-1}) trade-wind conditions the flow around Haleakala (model height H = 2,800 m) will have Fr ~ 0.25 with mountain tops well above the trade-wind inversion (~ 2 km) whereas the West Maui Mountains under normal trade-wind conditions and a model mountain height of 1,300 m will experience Fr ~ 0.54. With mountain heights well below the trade-wind inversion, the flow regimes over the West Maui Mountains differ from that over Haleakala as trade-wind flow aloft can move over the mountains (Schar and Smith 1993).

In the past, the Maui Vortex is suggested to form as a result of orographic effects and daytime heating (Leopold 1949; Ueyoshi et al. 1996) under trade-wind conditions and is more pronounced when trades are stronger (Ueyoshi et al. 1996). It is postulated that the low-level trade-wind flow is channeled through the central Maui Valley between the West Maui Mountains and Haleakala volcano; the flow then is diverted eastward by a combination of flow deflection by the West Maui Mountains and the daytime anabatic winds on the lee side slopes of Haleakala volcano with a closed vortex ciruclation over the Central Valley (Leopold 1949; Ueyoshi et al. 1996; Kodama and Businger 1998). The vortex circulation is most significant at the 1-km level with a return to the trade-wind flow at the 2-km level (Leopold 1949). Numerical simulations by Ueyoshi et al. (1996) suggest that the Maui Vortex may exist at night with a much weaker circulation. The importance of the Maui Vortex is its ability to trap pollutants due to agricultural burning which makes this an important feature for the forecasters at the Honolulu Forecast Office (Schroeder 1993; Kodama and Businger 1998). In addition, a strong vortex eddy can adversely affect aviation traffic to Kahului Airport located within the northern portion of the Central Valley.

In the previous modeling studies, the land surface forcing is either not considered or only crudely estimated. The objective of this work is: 1) to compare the simulated surface parameters from the MM5/LSM model (Yang et al. 2005) with surface observations; and 2) use the MM5/LSM model as a tool to study the effects of orographic blocking and land surface forcing on the development of the Maui Vortex over the Central Valley throughout the diurnal cycle.

---

* ***Corresponding author address*: DaNa L. Carlis, National Centers for Environmental Prediction, Environmental Prediction Center, Camp Springs, MD 20746; email: dana.carlis@noaa.gov**

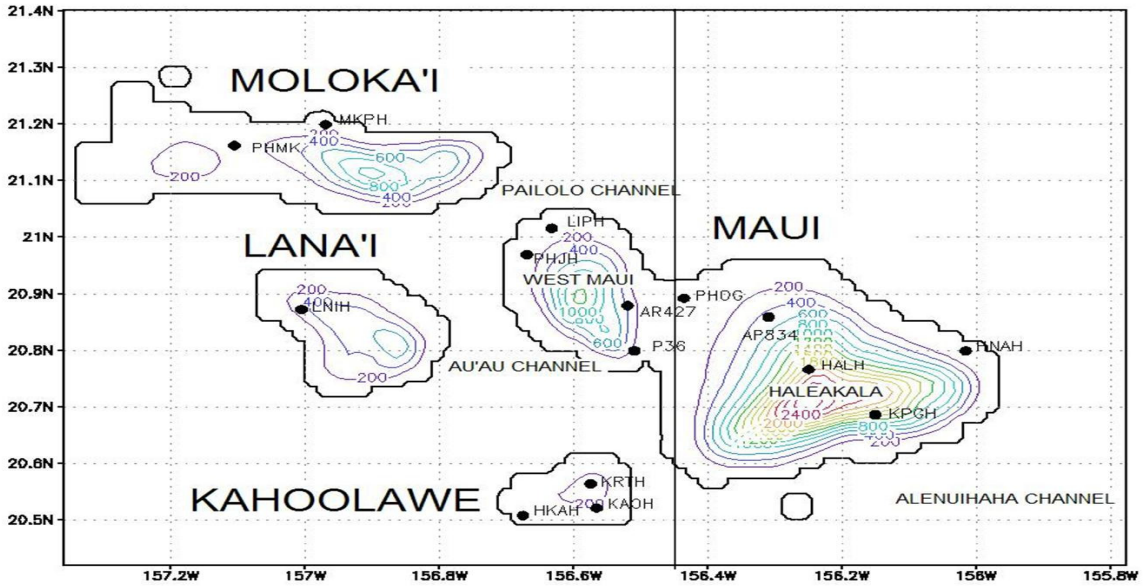

Figure 1. Map of Maui County showing station locations, mountains, and island terrain (200 m contours). Maui stations are LIPH, PHJH, PHOG, AR427, P36, AP834, HALH, KPGH, and HNAH. Molokai stations are MKPH and PHMK. The Lanai and Kahoolawe stations are LNIH, KRTH, KAOH, and HKAH. Straight line represent the vertical cross-section shown in Figure 6.

This work focuses on the 62-day mean daytime (1400 HST) and nighttime (0500 HST) flow regimes during a two-month simulation period of July and August 2005.

2. MM5/LSM model description and initialization

In this project, the PSU/NCAR MM5 (Dudhia 1993) is coupled with the National Centers for Environmental Predictions (NCEP), Oregon State University, Air Force, and NWS Office of Hydrology (NoaH) Land Surface Model (LSM) (Chen and Dudhia 2001). A LSM is necessary for the Hawaiian Islands due to heterogeneity of ground cover ranging from tropical rainforest on the windward slopes to bare lava rock in the lee. The original MM5 for Maui only has two vegetation types, mixed forest and urban, and three soil types, silt loam, clay, and clay loam. In this study, the 30″ resolution (~1 km) vegetation type, soil type, and vegetation fraction compiled by Zhang et al. (2005) (hereafter Z05) are used. The MM5-LSM model employs two-way nesting at horizontal resolutions of 54-km, 18-km, 6-km, and 2-km. The model's initial conditions are from the daily Global Forecast System (GFS). The resolution of the GFS is 1° x 1°. The high resolution global SST analysis with a 0.5° x 0.5° resolution from NCEP is used as the lower boundary conditions over the ocean. We employed 36 sigma levels from the surface to the 100-hPa level with 13 levels below sigma = 0.9. High vertical resolution is needed at the lower levels to resolve mountain winds and nocturnal inversion in the near surface layer (Chen and Feng 2001).

Similar to Z05 and Yang et al. (2005), prior to the study period, the MM5/LSM initialized at 0000 UTC using GFS output was run once per day for two months. The 24-hr forecast of soil parameters from the previous day's run are used as initial conditions at the lower boundary over land. Starting July 1, 2005, the 0000 UTC experimental forecast each day is archived on a 48-node Linux cluster. The model archive covered a 36-hour forecast with the results from the 12th through the 36th hour used to represent the diurnal cycle.

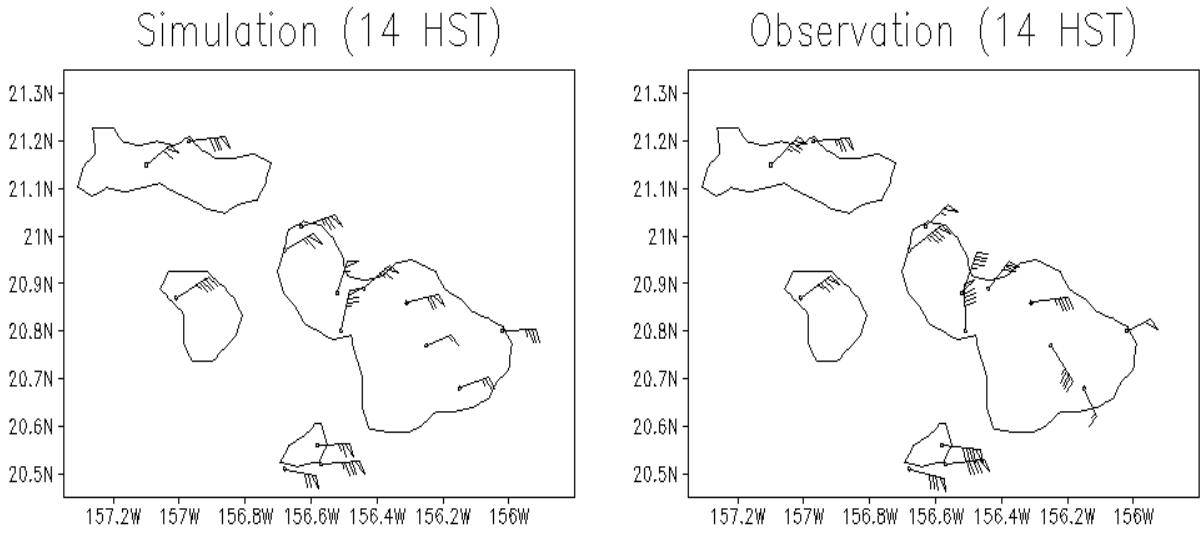

Figure 2. Mean map of stations across Maui County at 1400 HST comparing simulations (left) vs. observations (right). Wind barbs are valued as a pennant (5 m s^{-1}), full barb (1 m s^{-1}), and half barb (0.5 m s^{-1}).

3. Validation of the MM5/LSM

In Table 1 and 2, we show the mean 0500 HST and 1400 HST 2-m temperature statistics from stations across Maui County. At night, the model maintains a warm bias and a root-mean-square-error (RMSE) of 1.9 ℃. During the day, the MM5/LSM is slightly too cool with a RMSE of 2.6 ℃. The errors are slightly larger than Yang et al. (2005). A careful examination of the observed temperature data revealed that part of the discrepancies may be attributed to uncertainties in temperature measurements at a few sites that have relatively large differences between observed and simulated surface air temperatures.

Tables 1 and 2. 1400 HST and 0500 HST mean simulated and observed statistics of 2-m temperature for all stations with available data across Maui County.

1400 HST	2-m Temperature (°C)
Mean Simulation	26.46
Mean Observation	27.88
Bias	-1.42
Mean Absolute Error	2.09
Root Mean Square Error	2.62

0500 HST	2-m Temperature (°C)
Mean Simulation	22.70
Mean Observation	22.19
Bias	0.51
Mean Absolute Error	1.47
Root Mean Square Error	1.93

Horizontal distributions of mean observed and simulated winds for Maui County at 1400 and 0500 HST are shown in Figure 2 and Figure 3, respectively. At 1400 HST, the deflection of the decelerating incoming flow around the mountains over West Maui (AR427 and LIPH) is well simulated by the MM5-LSM. There are two stations within the Central Valley, Kahului International Airport (PHOG) along the northern portion of the valley and Maalaea Bay (P36) towards the southeastern portion. During the day, the simulated wind speed at PHOG is slightly lower than observed. Maalaea Bay is one of the windiest regions throughout the Hawaiian Islands, and the relatively strong winds there (~7.5 m s^{-1}) are well simulated. The simulated wind directions at both PHOG and P36 are in good agreement with observations. At Hana Airport (HNAH) on the windward side of Haleakala, the simulated wind speeds are lower than observed. The largest discrepancies between simulated and observed winds occur at Kaupo Gap (KPGH) on the southeastern slope of Haleakala.

The islands of Molokai, Lanai, and Kahoolawe are affected by airflow deflected by Maui. For example, the island of Kahoolawe is downstream of strong winds in the Alenuihaha Channel between East Maui and Northwest Hawaii with relatively large wind speeds that are simulated by the MM5/LSM rather well. The northeasterly winds observed at MKPH on the windward side of Molokai are reproduced by the model. The largest discrepancies (~2.5 m s^{-1}) were simulated at ARMI in the lee of Haleakala.

At 0500 HST, the MM5/LSM simulates the effects of nighttime cooling on airflow over the Maui County rather well. The flow splitting and deceleration on the windward sides of both Haleakala (e.g., HANA) and West Maui Mountain (AR427 and LIPH) are more significant compared to the daytime flow regime and are well simulated (Fig. 3). At KPGH on southeastern Maui, and AR834 on the lee slope of Haleakala, as well as AR427 on the eastern lower slope of the West Maui Mountains, the nighttime flow has a downslope wind component. This feature is well simulated by the MM5/LSM. However, the model tends to overestimate the downslope/katabatic flow on the slope. At PHMK on Molokai, the model displays westerly airflow when the observation specifies northeasterly trade-wind flow at night.

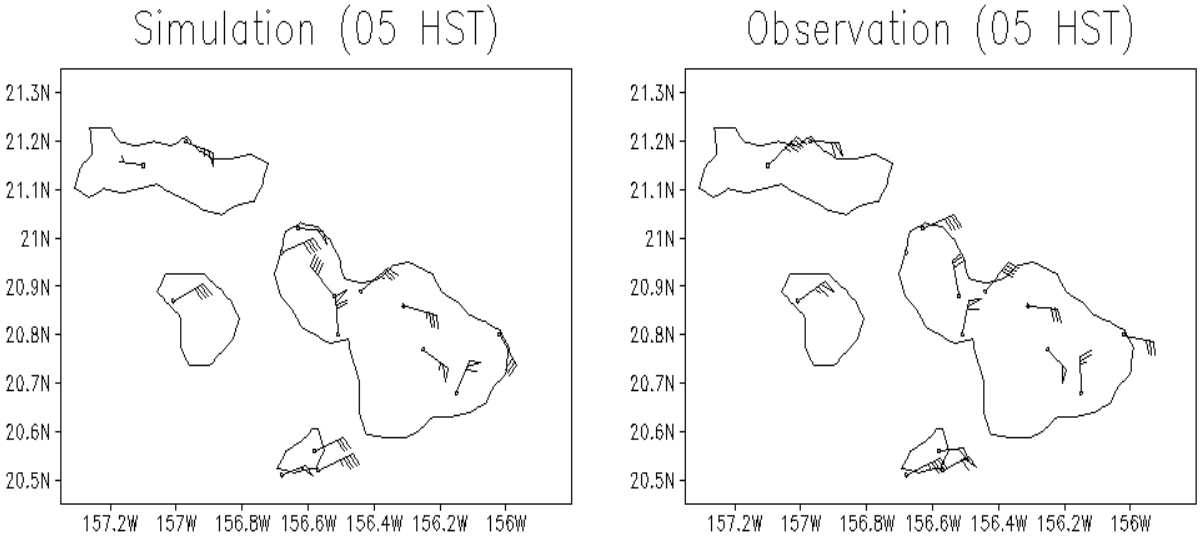

Figure 3. Mean map of stations across Maui County at 0500 HST comparing simulations (left) vs. observations (right). Wind barbs are valued as a pennant (5 m s^{-1}), full barb (1 m s^{-1}), and half barb (0.5 m s^{-1}).

4. Diurnal effects on island-scale airflow and the Maui Vortex

Hourly model results for the simulation period are averaged for each hour throughout the diurnal cycle. This section describes the mean daytime (1400 HST) and nighttime (0500 HST) flow regimes over the Maui County and the Maui Vortex at the surface and the 1-km level.

4.1. Island-scale airflow at 1400 HST

On the windward side of Haleakala, the velocity of the incoming northeasterly trade-wind flow is ~ 7 m s^{-1} during the day. As the trade-wind flow moves toward the island, airflow decelerates drastically to ~ 3 m s^{-1} along the northeastern windward coast near Hana as a result of orographic blocking (Fig. 4a). The incoming decelerating trade-wind flow exhibits splitting airflow over the windward lowlands (< 2 m s^{-1}). On the southeastern and western lee side slopes, the surface airflow exhibits anabatic/upslope winds as a result of daytime heating. Incoming airflow over the West Maui Mountains differs slightly as the trade-wind flow aloft moves over the top of the mountain due to the mountains' residence below the inversion layer. A weak onshore flow is present along the lees-die coast.

Winds over the Maui Central Valley are relatively strong (≥ 6 m s^{-1}) with a wind speed maximum around the corners of the West Maui Mountains. A well defined closed vortex circulation is apparent over the Central Valley (or the Maui Vortex) between the strong northeasterly/northerly winds channeled between Haleakala and the West Maui Mountains and westerly anabatic winds on the western lee side slopes of Haleakala volcano.

The southeastern coast is another region with strong winds as the southern branch of the splitting airflow on the windward side is forced to move around Haleakala with the strongest winds within the Alenuihaha Channel off the coast. On the southwestern lee side corner of Haleakala, anticyclonic horizontal shear is present between the strong winds along the southeastern coast and the westerly anabatic winds in the lee of Haleakala.

At the 1-km level, the winds are strong (> 12 m s^{-1}) over the Alenuihaha and Pailolo Channels (Fig. 4b). Over the island of Maui, strong winds are simulated over the Central Valley (≥ 8 m s^{-1}) and along the southeastern coast (≥ 12 m s^{-1}). A westerly return flow is apparent in the lee of Haleakala at the 1-km level. The northern cyclonic lee vortex is more pronounced with a larger horizontal extent than the southern anticyclonic lee vortex, perhaps due to the shape of Haleakala volcano. The impinging angle of the incoming trade-wind flow with the terrain contours is relatively large for the northeastern slopes of Haleakala as compared with that of the southeastern. Over the West Maui Mountains, strong downslope winds are simulated on the southwestern and southeastern corners as the airflow aloft moves over the ridge line and descends in the lee.

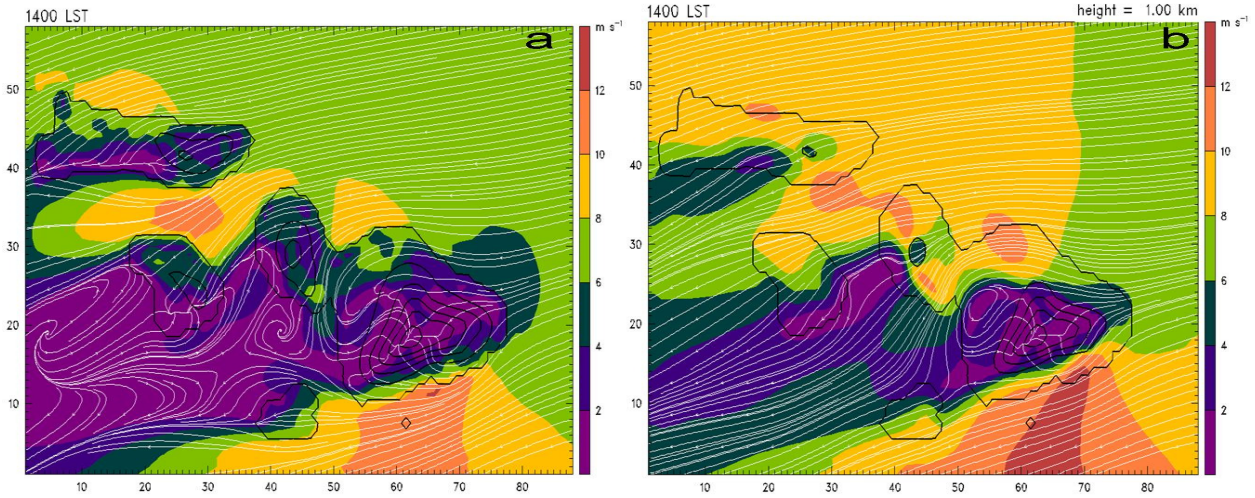

Figure 4. Mean 1400 HST horizontal streamline maps at 10-m (a) and 1.0-km (b) from the 2-km MM5/LSM during summer trade-wind conditions. Wind speeds are shaded every 2 m s^{-1} and terrain contours are every 500 m (terrain contours for 1.0-km map begin at 1.0-km in elevation).

4.2. Island-scale airflow at 0500 HST

For the nighttime flow regime, surface winds are rather weak (< 4 m s^{-1}) over most of Maui, Molokai and Lanai except the southwestern and southeastern corners of the West Maui Mountains (Fig. 5a). The flow splitting along the windward coasts of Haleakala volcano and the West Maui Mountains is more significant than during the daytime flow regime with katabatic winds on the slopes around the Haleakala volcano and the windward side of the West Maui Mountains. The wind speed minimum over the Central Valley is less than 2 m s^{-1}. The downslope winds off the Maalaea Bay in the lee of West Maui Mountains are stronger than during the daytime.

A closed weak vortex circulation exists over the Central Valley between the winds moving around the northern corner of Haleakala and weak katabatic winds on the lee side slopes of Haleakala volcano. Northwesterly winds off the windward slopes of West Maui trap the vortex of the Central Valley. The wake in the lee of Haleakala extends southwestward covering the Island of Kahoolawe.

At the 1-km level (Fig. 5b), strong winds are simulated along the southeastern coast and the northern corner of Haleakala volcano with a westerly return flow in the lee of Haleakala. Dual counter-rotating lee vortices with a westerly flow between the vortices are simulated. Over the West Maui Mountains, strong downslope winds are simulated on the lee side slopes with dual-counter rotating vortices at 0.5-km over the Auau Channel between West Maui and Lanai (not shown).

The daytime and nighttime vertical cross-sections (Fig. 1) of the u-component of the wind over Central valley are shown in Figures 6a and 6b, respectively to study the vertical extent of the westerly return flow in the lee of Haleakala. Strong horizontal cyclonic and anticyclonic shear to the north and south of the Central Valley with a weak (~2 m s^{-1}) westerly return flow in the lee are present at both times as a result of orographic blocking by Haleakala volcano. The westerly return flow extends well above the 1.5-km level and is present throughout the diurnal cycle. It is apparent that the Maui Vortex is mainly of orographic blocking with counter-rotating vortices in the lee. However, the northern cyclonic vortex is more pronounced with a larger horizontal extent than the southern because of the shape of Haleakala volcano. In the lowest levels, these vortices are modified by lower-level airflow driven by the diurnal heating cycle and the orographic blocking by the West Maui Mountains.

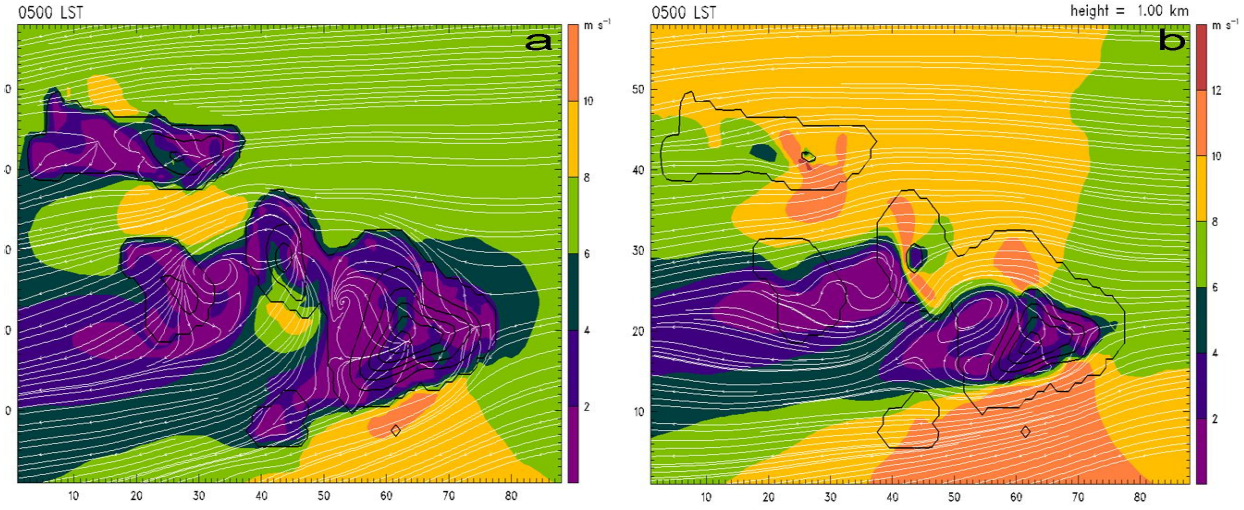

Figure 5. Mean 0500 HST horizontal streamline maps at 10-m (a) and 1.0-km (b) from the 2-km MM5/LSM during summer trade-wind conditions. Wind speeds are shaded every 2 m s^{-1} and terrain contours are every 500 m (terrain contours for 1.0-km map begin at 1.0-km in elevation).

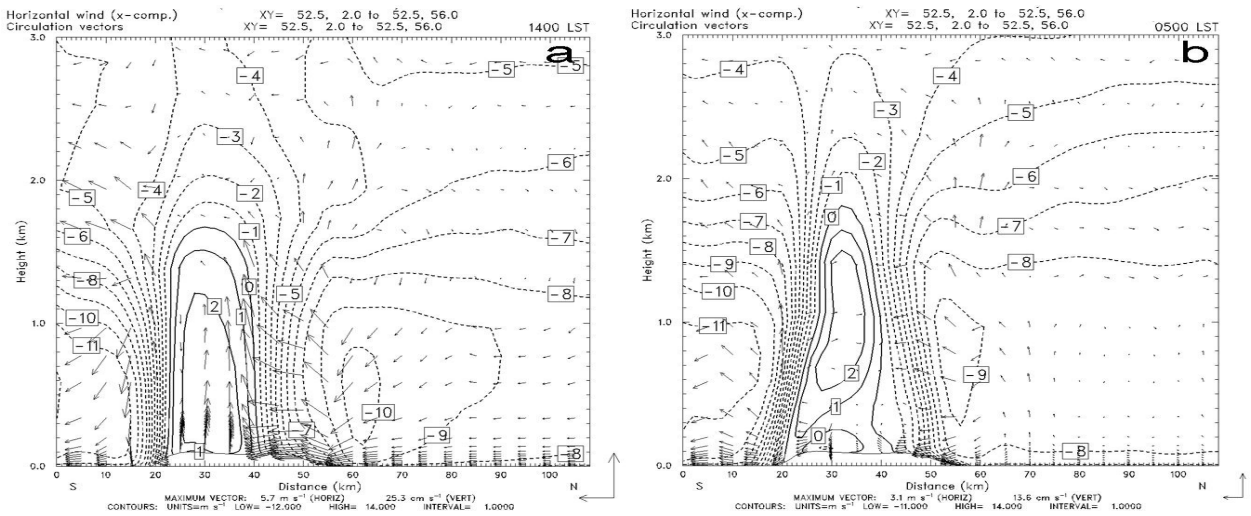

Figure 6. Vertical N-S cross-section (Fig. 1) of the u-component wind speed (m s^{-1}) contours and circulation vectors along the north-south gradient of the Central Valley of Maui at 1400 (a) and 0500 (b) HST.

5. Summary

In closing, the MM5/LSM shows skill in predicting orographic airflow patterns past the island of Maui under summer trade-wind conditions. Horizontal airflow maps show that island-scale airflow past Maui is influenced by island blocking, flow splitting, upstream flow deceleration, and the diurnal heating/cooling cycle.

For Haleakala volcano with heights well above the trade-wind inversion, the wake at the 1-km level is dominated by dual counter-rotating vortices above the surface with a westerly return flow in the lee during the daytime and at night. The northern cyclonic lee vortex (known as the Maui Vortex) is more pronounced with a larger horizontal extent than the southern anticyclonic lee vortex, perhaps due to the shape of Haleakala volcano. The impinging angle of the incoming trade-wind flow with the terrain contours is relatively large for the northeastern slopes of Haleakala as compared with that of the southeastern slopes. The angle of the incoming airflow effects the formation of a closed anticyclonic circulation throughout the diurnal cycle.

At the surface, the airflow over Maui's Central Valley is strongly modulated by the diurnal heating cycle and also affected by the airflow induced by the West Maui Mountains. During the daytime, the northern counter-rotating vortex is enhanced by strong winds channeled through the valley and the development of anabatic winds on the western lee side of Haleakala with a closed circulation. In contrast, with the anabatic winds on the lee side slope, the southern counter vortex is degraded with the streamline chart showing a slightly closed circulation. At night, the surface flow around the slopes of Haleakala volcano and the eastern slopes of the West Maui Mountains is dominated by katabatic winds. Winds over the Central Valley are relatively calm as compared with the daytime. As a result, the dual counter-rotating lee vortices due to blocking of trades by Haleakala volcano are not evident at the surface; however, above the surface the dual vortices return over the Central Valley.

For the West Maui Mountains with tops below trade-wind inversion, the airflow aloft is able to move over the mountain top and descend in the lee. The flow splitting on the windward side at the surface and the downslope winds on the lee side slopes are more significant at night than during the day. During the daytime, weak onshore flow is simulated along the lee side coast whereas at night, dual-counter rotating vortices are simulated in the wake offshore at the 0.5-km level.

We are in the process of shifting our modeling basis from the MM5 to the Weather Research and Forecasting Model (WRF). In addition, we would like to improve initial conditions of our regional domain by assimilating unconventional data. The WRF/LSM model will also be used as a research tool to study the local effects for high impact weather events such as heavy-rainfall and high-wind events.

6. References

Chen, Y.-L., and J. Feng, 2001: Numerical simulations of airflow and cloud distributions over the windward side of the island of Hawaii. Part I: The effects of trade-wind inversion. *Mon. Wea. Rev.*, **129**, 569-585.

—, and J. Dudhia, 2001: Coupling an advanced land surface – hydrology model with the Penn State – NCAR MM5 modeling system. Part I: Model implementation and sensitivity. *Mon. Wea. Rev.*, **129**, 569-585.

Dudhia, J. 1993: A nonhydrostatic version of the Penn State-NCAR mesoscale model: validation tests and simulation of an Atlantic cyclone and cold front. *Mon. Wea. Rev.*, **121**, 1493-1513.

Leopold, L. B., 1949: The interaction of trade-wind and sea breeze, Hawaii. *J. Meteor.*, **6**, 312-320.

Kodama, K. R., S. Businger, 1998: Weather and forecasting challenges in the Pacific region of the National Weather Service. *Wea. Forecasting*, **13**, 523-544.

Schär, C., and R. B. Smith, 1993: Shallow-water flow past isolated topography. Part I: Vorticity production and wake formation. *J. Atmos. Sci.*, **50**, 1373-1400.

Schroeder, T. A.,1993: *Climate Controls. Prevailing Trade-winds*. M. Sanderson, Ed., University of Hawaii Press, 12-36.

Smolarkiewicz, P. K., R. M. Rasmussen, and T. L. Clark, 1988: On the dynamics of Hawaiian cloud bands: Island forcing, *J. Atmos. Sci.*, **45**, 1872-1905.

—, and R. Rotunno, 1989: Low Froude number flow past three-dimensional obstacles. Part I: Baroclinically generated lee vortices. *J. Atmos. Sci.*, **46**, 1154-1164.

Ueyoshi, K., J. O. Roads, F. Fujioka, and D. E. Stevens, 1996: Numerical Simulation of the Maui Vortex in the trade-winds. J*. Meteor. Soc. Japan*, **74**, 723-744.

Yang, Y., Y.-L. Chen, and F. Fujioka 2005: Numerical simulations of the island-induced circulations over the island of Hawaii during HaRP. *Wea. Forecasting*, **133**, 3693-3713.

Zhang, Y., Y.-L. Chen, S.-Y. Hong, K. Kodama, and H.-M. H. Juang, 2005: Validation of the coupled NCEP Mesocale Spectral Model and an advanced Land Surface Model over the Hawaiian Islands. Part I: Summer trade-wind conditions over Oahu and Heavy rainfall events. *Wea. Forecasting*, **20**, 847-872.